Modeling of Casting, Welding and Advanced Solidification Processes X
Edited by D.M. Stefanescu, J. Warren, M. Jolly and M. Krane
TMS (The Minerals, Metals & Materials Society), 2003

STUDY OF THE RHEOLOGY OF SEMISOLID ALLOYS WITHIN A CAPILLARY VISCOMETER

A. Ludwig, M. Wu, M. Fehlbier, C. Afrath and A. Bührig-Polaczek

Foundry Institute, Aachen University, Intzestr. 5, D-52072 Aachen, Germany

Abstract

Semisolid alloy exhibits a shear rate history dependent flow behavior. The increasing interest on numerical modeling of the thixo-casting process makes it quite important to understand the flow behavior of semisolids. Its viscosity is the key parameter for any numerical model of this process. In this paper a two phase approach is used to investigate the rheology of semisolid alloys. It is assumed that both liquid and solid phases can be regarded as interpenetrating continua with their own viscosities. The flow field within an capillary viscometer used to experimentally investigate the viscosity of semisolids is simulated. The results show that the rheology of the two phase flow is determined by the interaction between the solid and the liquid in particular the momentum exchange between the two phases. Apparent non-Newtonian flow behavior of the solid-liquid mixture is predicted, although both phases are considered as Newtonian fluids. The occurrence of phase separation and concentration inhomogeneity within the capillary viscometer is also discussed.

Introduction

An engineering viscometer (Fig. 1) is traditionally used to determine the viscosity of a semisolid[1,2]. The semisolid slurry with a constant volume flow rate $Q(=\bar{u}\cdot H\cdot W)$ is pressed through a capillary tube, where $\bar{u}$ is the average velocity of the slurry, H is the height and W is the width of the capillary tube ($W >> H$). When the flow comes to a steady state the pressure drop Δp along the tube length L is experimentally measured. Hence, the true shear stress at the tube wall τ_w can be determined by

$$\tau_w = \frac{H\cdot\Delta p}{2\cdot L}. \tag{1}$$

The apparent shear rate γ_{ap} is

$$\gamma_{ap} = \frac{6\cdot Q}{W\cdot H^2} \tag{2}$$

Considering the non-Newtonian flow behavior in the tube, the true shear rate γ_w is obtained with the following modification[1].

$$\gamma_w = \frac{\gamma_{ap}}{3}\cdot\left(2+\frac{\tau_w}{\gamma_{ap}}\cdot\frac{d\gamma_{ap}}{d\tau_w}\right) \tag{3}$$

The mixture viscosity μ_{mix} (or the true viscosity μ_w) of the slurry is defined as

$$\mu_{mix} = \frac{\tau_w}{\gamma_w}. \tag{4}$$

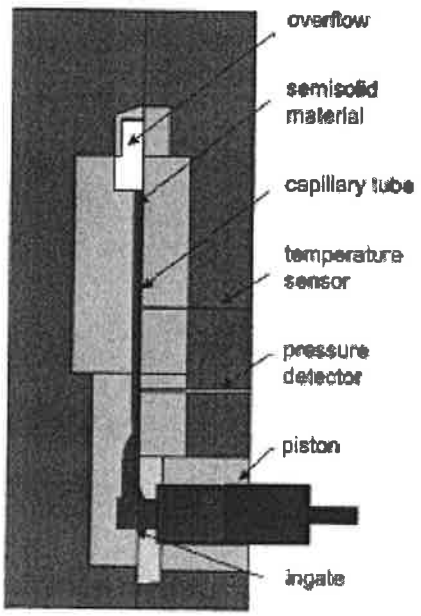

Figure 1. Capillary Viscosimeter[1].

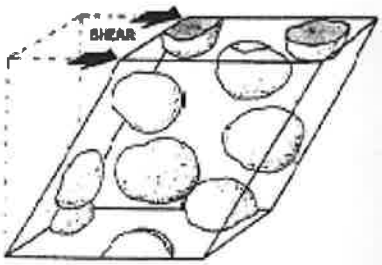

Figure 2. Rheological behavior of a volume

element of semisolid material.

According to this measurement, the viscosity of a solid-liquid mixture is proportional to the measured pressure drop Δp and inversely proportional to the steady state flow rate Q. Experimental studies indicate that the viscosity of a semisolid varies over a very wide range, depending on grain structure, fraction of solid, and other process parameters.

In order to gain a deep understanding of the experimental results a closer look to the thixotropic rheology of semisolid materials is needed. When an alloy that normally solidifies dendritically is vigorously stirred during solidification, the dendritic structure can be broken up and be replaced by a more-or-less spherical structure (Fig. 2)[3]. The semisolid slurry injected into a thixo-casting die has nearly spherical solid particles suspended in a liquid matrix[4]. Based on this fact, a two-phase approach is used to investigate the flow behavior of the semisolid alloy, and thus to achieve understanding of the shear-rate history dependent rheology. The applied two phase model was previously used to study the microstructure formation and segregation phenomena during solidification[5-9].

Two phase model

The semi-solid slurry is characterized by two phases: liquid and solid. In the two-phase flow model it is assumed that both liquid and solid are described as two inter-penetrating Newtonian continua. Thus, both phases have quantities like velocity $\vec{u}_l$ and $\vec{u}_s$, volume fraction α_l and α_s, density ρ_l and ρ_s, and viscosity μ_l and μ_s. They are coupled by the constrain

$$\alpha_l + \alpha_s = 1 \tag{5}$$

and by considering a momentum exchange between the two phases. As a fictitious parameter the viscosity of the solid μ_s stands for the interaction between the dispersed grains among themselves. The conservation equations of mass and momentum for both liquid and solid ($q = s$, l) are formulated as

$$\frac{\partial}{\partial t}(\alpha_q \rho_q) + \nabla \cdot (\alpha_q \rho_q \vec{u}_q) = 0 \tag{6}$$

$$\frac{\partial}{\partial t}(\alpha_q \rho_q \vec{u}_q) + \nabla \cdot (\alpha_q \rho_q \vec{u}_q \otimes \vec{u}_q) = -\alpha_q \nabla p + \nabla \cdot \bar{\bar{\tau}}_q + \alpha_q \rho_q \vec{g} + \vec{U}_{pq} \tag{7}$$

with the stress tensor

$$\bar{\bar{\tau}}_q = \alpha_q \mu_q \left(\frac{\partial u_{q,i}}{\partial x_j} + \frac{\partial u_{q,j}}{\partial x_i}\right) - \frac{2}{3}\alpha_q \mu_q \delta_{ij} \frac{\partial u_{q,l}}{\partial x_l}. \tag{8}$$

The most important term in these equations is the momentum exchange

$$\vec{U}_{pq} = K_{pq}(\vec{u}_p - \vec{u}_q). \tag{9}$$

The momentum exchange coefficient K_{pq} is given by the Kozeny-Carman approach[10]

$$K_{pq} = -180\frac{\mu_q}{d_p^2}\frac{\alpha_p^3}{\alpha_q} \qquad (10)$$

Here d_p is the average diameter of the disperse phase, i.e. the average diameter of the solid grains. According to this momentum exchange model it is clear that for a given solid fraction a small grain size leads to a large momentum transfer (strong coupling), whereas a large grain size leads to a small momentum exchange between liquid and solid (loose coupling).

Problem definition and calculation procedure

A two-dimensional configuration, similar to a cross-section of the experimental capillary tube shown in Fig. 1, with a length L of 400 mm and a height H of 4 mm is considered. The numerical domain is divided into 20 x 400 volume elements. It is assumed that the flow is isothermal, the fraction of solid entering the domain is constant ($\alpha_s = 0.5$) and no phase change (no solidification or remelting) occurs during the process. As an initial condition the whole capillary tube is supposed to be filled with non-moving liquid. The fluid-wall interface is treated as no-slip boundary. At the outlet a zero diffusion flux condition is applied. The material properties and the other geometrical parameters used in the simulations are listed in Table I.

Table I: Thermal physical properties and other parameters considered in the model.

Density of the liquid	ρ_l	2606 kg/m^3	length of tube	L	400 mm
Density of the solid	ρ_s	2743 kg/m^3	height of tube	H	4 mm
Viscosity of the liquid	μ_l	$1.3\cdot10^{-2}$ kg/(m·s)	grids in length direction		400
Viscosity of the solid	μ_s	$10^{+2} - 10^{+2}\ \mu_l$	grids in height direction		20
Average grain size	d_s	1 - 200 µm	solid fraction	α_s	50%
Inlet velocity	V_0	0.01 - 10 m/s			

With the above presented two-phase model the pressure drop along the capillary tube is numerically calculated. The mixture viscosity μ_{mix} of the semisolid slurry is then estimated by using the same procedure as for the experimentally used capillary viscometer[1], which is described by Eq. (1)-(4). By varying the parameters of the grain diameter d_s and the inlet velocity V_0, the relation between the mixture viscosity μ_{mix} and the shear rate $\dot{\gamma}$ is obtained. Phase separation phenomenon can be directly described with the phase distribution α_s, which is obtained by solving the mass conservation equation Eq. (6).

Results and discussions

Rheology

A typical simulation result is schematically shown in Fig. 3. The pressure field is shared by both liquid and solid, but both phases have their own velocity profiles. Due to the inlet effect it takes some time for both phases to develop a steady state parabolic velocity profile along the capillary tube. In this transient zone the velocity profile is non-parabolic. An important feature of the transient zone is that the pressure drop along the tube axis is not linear as it is in the developed zone (Fig. 4). The theoretical consideration on which the viscosity estimation using the capillary viscometer is based on, is the assumption that a linear pressure drop along the tube occurs. However, a non-linear pressure drop is predicted in the transient zone near the inlet. The length of this zone is strongly influenced by the inlet velocity. If the inlet velocity is small for

example 0.01 m/s, the transient zone tends to (practically) zero. If the inlet velocity is large, for example 10 m/s, the transient zone is quite extended. In order to get reasonable measured viscosity data a long transient inlet zone is inadmissible. Thus, the inlet velocity should be appropriately small, or the two pressure sensors should be carefully located to avoid the transient zone, especially when large inlet velocities are applied. In any case it should be ensured that the pressure gradient between the pressure sensors is reasonably linear.

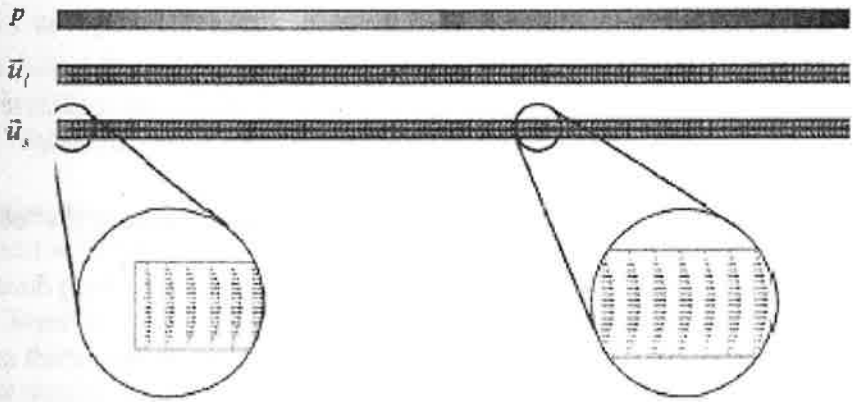

Figure 3. Typical results of a two-phase flow simulation in the capillary tube: pressure distribution, p, velocity field of liquid and solid, $\vec{u}_l$ and $\vec{u}_s$. Note that at the inlet a transient zone is present where the velocity fields change from being uniform into being parabolic (left insert). Beyond this transient zone a steady-state flow pattern establishes (right insert).

The different velocity profiles of the liquid and the solid are caused by the different viscosities assumed in the numerical model. Torque stirring experiments on the solidifying aluminum alloys[11] have shown that the shear stress of the solidifying semisolid slurry increased sharply at the coherency point, at which the solid grains starts to impinge each other. The fraction solid at the coherency point varies between 0.1 for poorly grain refined alloys and 0.5 for fine grain alloys. In our simulation we considered $\alpha_s = 0.5$ which is supposed to be beyond the coherency point. Therefore a significant high viscosity ($100 \cdot \mu_l$) is chosen for the solid phase. On the other hand, the difference of the velocity profiles caused by the different viscosities of both phases is leveled out by the influence of a high drag force. When the particle size is small (e.g. 1 μm), a large momentum exchange coefficient K_{sl} is obtained (see Eq. (10)) and the two phases are strongly coupled. Thus, the velocity profiles of both phases are quite equal independent of the different viscosities. If the particle size is large (e.g. 200 μm), a distinct difference of the velocity profiles is observed. It is implied that with large grains a phase separation more likely occurs because both phases are loosely coupled and different velocity profiles are possible.

Fig. 5 shows the mixture viscosity of the semisolid as a function of shear rate. In an ideal Newtonian fluid the viscosity is independent of the shear rate. But here a shear-rate dependent viscosity is obtained. Although both the liquid and solid are assumed to be of Newtonian fluid, the two-phase approach is able to describe a non-Newtonian behavior for the mixture. Since in the present two-phase model the liquid-solid coupling is realized by only the momentum exchange term, it indicates that the non-Newtonian phenomena of the semisolid may be understood as an interaction between the two phases. In Fig. 5 the influence of the momentum exchange strength (via grain size) on the non-Newtonian behavior is shown. Our study implies that the semisolid slurry with small momentum exchange between the two phases (large grain size) produces a strong non-Newtonian behavior.

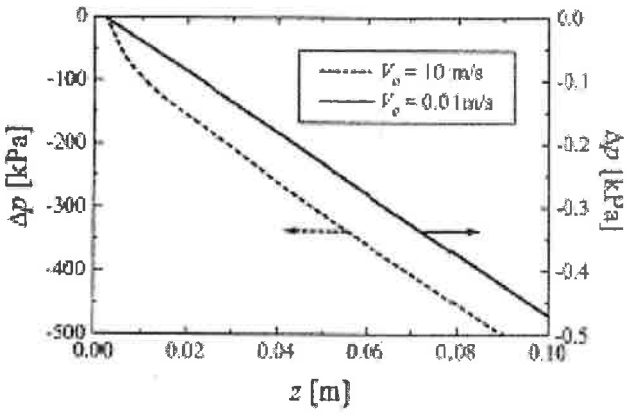

Figure 4. Effect of inlet velocity on the pressure distribution along the tube.

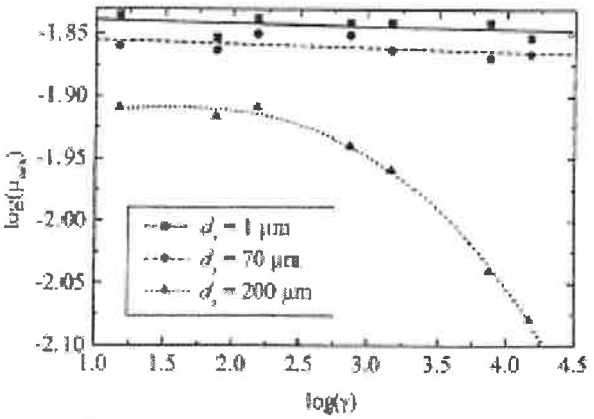

Figure 5. Numerically predicted mixture viscosity of the semisolid (μ_{mix}) as function of shear rate γ.

Also in experiments the shear-thinning behavior (decreasing viscosity with increasing shear rate) is found[3,4]. This shear-thinning phenomenon was believed to attribute to the formation and fragmentation of particle agglomerates[4,12]. Solid particles are prone to agglomerate by 'welding process' during collisions, which then trap liquid within the agglomerate, resulting in higher effective solid fraction and viscosity. With increasing shear rate the agglomerate size decreases resulting in lower apparent viscosity. In our two-phase model the agglomeration-and-fragmentation effect was not taken into account. Nevertheless, for large grain sizes a shear rate dependent viscosity is predicted even without those agglomeration and fragmentation effects.

The determination of the viscosity of a semisolid following literature[1] is based on the assumption of a non-slip boundary condition for both phases. However, there are evidences showing that the assumption of non-slip is not adequate for the solid phase[2]. We are planning to modify our model by considering the solid phase to slip along the tube walls.

Phase separation

Fig. 6(a) shows the phase separation process near the inlet region. Before entering into the inlet the semisolid mixture is assumed to be uniform with α_s =0.5. By passing through the transient zone a 'M' shape phase distribution is established, Fig. 6(b). Near the capillary wall the fraction solid α_s is relatively low, 0.4905, while about 0.5 mm from the capillary wall a strip of solid

enriched zone with α_s =0.5024 forms. In the capillary center the phase is uniformly distributed with α_s near to or a little lower than 0.5. From the modeling results it becomes clear that the phase separation in the capillary viscometer occurs in the transient zone. After the transient zone the phase distribution profile across the capillary tube remains unchanged.

The phase separation process in the transient zone can be made visible by the relative velocity field $\Delta\vec{u} = \vec{u}_l - \vec{u}_s$ as shown in Fig. 6(c). Just near to the inlet and capillary wall the $\Delta\vec{u}$ points to the wall, causing enrichment of liquid phase (i.e. depletion of α_s) on the surface region. About 5 mm away from the wall the $\Delta\vec{u}$ points gradually to the capillary center. This kind of $\Delta\vec{u}$ profile indicates that there exists a zone (about 5 mm from the wall) where the liquid phase is depleted. Where the liquid phase is depleted the solid phase is enriched.

The mechanism for the $\Delta\vec{u}$ and the phase separation can be understood from the rheology of both liquid and solid phases and the interaction between them. A non-slip boundary condition is applied for each phase. The capillary wall try to 'brake' the velocity of both phases and build up a boundary layer in the transient zone. According to the boundary theory[10] the higher the viscosity, the thicker the boundary layer. In other words, the phase with lower viscosity (liquid) tends to flow straighter along the capillary tube and the velocity field of the phase with higher viscosity (solid) is more strongly deformed and try to build up a thicker boundary layer.

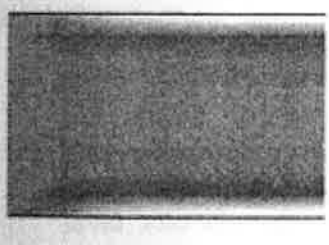

a) Solid phase α_s distribution near the inlet region (light 0.4905, dark 0.5024).

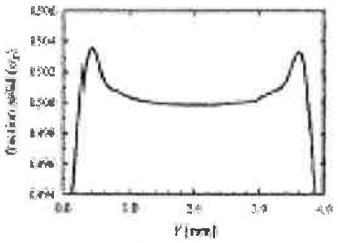

b) Solid phase α_s distribution profile across the capillary tube.

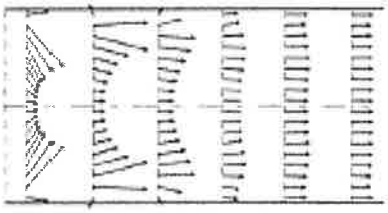

c) Relative velocity near the inlet region ($\Delta\vec{u} = \vec{u}_l - \vec{u}_s$).

Figure 6. Phase separation phenomenon in the viscometer (d_s = 70 μm, V_0 = 0.5 m/s).

The results presented in Fig. 6 (a) and (b) have not been evaluated by comparing with experiments. According to the above discussions factors influencing the phase separation include the rheology (viscosity) of the phases, the interaction (drag force) between them and even the boundary condition. Therefore, the presented numerical analysis should be understood as impulse for decided experimental studies.

With the phase separation the appearance of the concentration inhomogeneity (or macro-segregation) is straightforward. Generally the solid and the liquid phases have different concentrations. Relative movement between the two phases leads to macroscopic solute inhomogeneity. For example, an Al-4 wt% Cu alloy has solute (Cu) partitioning coefficient of $k < 1$. With the phase separation shown in Fig. 6(a), it is deduced that positive segregation (> 4 wt% Cu) would occur near the wall of the capillary tube, and negative segregation (< 4wt% Cu) in the region about 5 mm from the capillary wall. An experimental study of the macrosegregation on the semisolid capillary specimen would be a direct proof of the numerical prediction.

Conclusions

A two-phase model is used to describe a non-Newtonian behavior of the semisolid alloy. Although both liquid and solid are assumed to be of Newtonian fluid type and agglomeration and fragmentation effects are not considered, the two-phase approach predicts non-Newtonian flow behavior for the solid-liquid mixture. The coupling and the interaction (momentum exchange) of the two phases are responsible for the non-Newtorian behavior.

The numerical simulation shows the existence of a velocity-dependent transient zone near the inlet of the capillary tube. It implied that special care must be taken and the transient zone must be avoided when measuring the pressure gradient along the tube. The pressure gradient near the inlet is not linear especially when a large inlet velocity is applied.

Even in the geometry as simple as the capillary tube phase separation would occur. The non-slip boundary condition and the different viscosities of both liquid and solid phases result in a relative velocity field between the two phases. The relative velocity field leads to the phase separation. Macrosegregation (concentration inhomogeneity) is the direct result of this phase separation.

Acknowledgement

This work was financially supported by the German Science Foundation (DFG) as part of the collaborative research centers "Integral Materials Modeling" SFB 370 and "Forming of Metals in the Semi-Solid State and Their Properties" SFB 289, for which the authors wish to express their gratitude.

References

1. DIN 53014, Kapillarviskosimeter mit Kreis- und Rechteckquerschnitt zur Bestimmung von Fließkurven (Berlin: Beuth Verlag GmbH, 1992.6).
2. C.J. Paradies et al., in Proc. 4th Intern. Confer. Semi-Solid Processing of Alloys and Composites (Sheffield, June 1996), 115-119.
3. M. C. Flemings, in Proc. 3th Intern. Confer. Semi-Solid Processing of Alloys and Composites (Tokyo, June 1994), 3-6.
4. D. Ghosh, R. Fan, and C. VanSchilt, in Proc. 3th Intern. Confer. Semi-Solid Processing of Alloys and Composites (Tokyo, June 1994), 85-94.
5. A. Ludwig, and M. Wu, "Modeling of globular equiaxed solidification with a two phase approach," Metall. Mater. Trans. A 33A (2002), 3673-3683.
6. M. Wu, and A. Ludwig, "Influence of phase transport phenomena on macrosegregation and structure formation during solidification," Adv. Eng. Mater. Vol. 5 No. 1 (2003), in press.
7. A. Ludwig, G. Ehlen, M. Pelzer, P.R. Sahm, in Proc. McWASP IX, SIM2000, ed. P.R. Sahm et al. (Aachen: Shaker-Verlag, 2000), 175-182.
8. C. Beckermann, and R. Viskanta, Appl. Mech. Rev., 46(1993), 1-27.
9. C.Y. Wang, et al., Metall. Trans. B, 26B (1995), 111-.
10. R. B. Bird, W. E. Steward, and E. N. Lightfoot, Transport Phenomena, (New York: John Wiley & Sons, 1960).
11. L. Arnberg, G. Chai and L. Backerud, Mater. Sci. and Eng. 173A (1993), 101-103.
12. L. S. Turng and K. K. Wang, J. of Mter. Sci., 26(1991): 2173-2183.